Phase Behavior and Rheology of Polystyrene/Poly(α-methylstyrene) and Polystyrene/Poly(vinyl methyl ether) Blend Systems

Jin Kon Kim,* Hee Hyun Lee, and Hye Won Son

Department of Chemical Engineering and Polymer Research Institute, Pohang University of Science and Technology, Pohang, Kyungbuk 790-784, Korea

Chang Dae Han

Department of Polymer Engineering, The University of Akron, Akron, Ohio 44325

Received April 21, 1998

ABSTRACT: The phase behavior and rheology of binary blends of polystyrene (PS) and poly(α-methylstyrene) (PαMS), exhibiting upper critical solution temperature (UCST), and binary blends of PS and poly(vinyl methyl ether) (PVME), exhibiting lower critical solution temperature (LCST), were investigated. For the study, (i) PS-40/PαMS-18, (ii) PS-38/PαMS-39, (iii) PS-40/PαMS-48, and (iv) PS-110/PVME-95 blend systems were prepared by solution casting. The results of differential scanning calorimetry suggest that each blend system investigated is miscible over the entire blend composition as evidenced by the single composition-dependent glass transition temperature. However, from oscillatory shear rheometry we observed evidence suggesting that microheterogeneity is present in the miscible region, as determined by cloud point measurements, at temperatures as far away as approximately 70 °C above the UCST of the PS/PαMS blend system and at temperatures as far away as only approximately 7 °C below the LCST of the PS/PVME blend system. Such observation leads us to conclude that the extent of dynamical composition fluctuations near the critical point depends on the chemical structures of a polymer pair. The observed difference in the extent of dynamical composition fluctuations between PS/PαMS and PS/PVME blend systems is interpreted by the difference in the temperature coefficient of the interaction parameter between the PS/PαMS and PS/PVME blend systems.

Introduction

The rheological behavior of miscible and partially miscible polymer blends has been investigated extensively.[1−16] Often, a blend is regarded as being miscible when it exhibits a single glass transition temperature (T_g) and immiscible when it exhibits two distinct T_gs corresponding to the T_g of the constituent components.[17] More often than not, one observes a very broad, single glass transition in a pair of miscible polymers, as determined by differential scanning calorimetry (DSC). For instance, Schneider and Wirbser[15] have shown that some polystyrene (PS)/poly(vinyl methyl ether) (PVME) blends undergo a very broad (as much as 60 °C), single glass transition. A question may be raised as to whether or not a polymer pair can be regarded as being miscible on the segmental level (say less than approximately 5 nm) when a very broad, single glass transition is observed. This is due to the fact that a dynamic mechanical thermal analysis (DMTA) can resolve the size of domains (or separated phases) on the order of 5−10 nm[18] and DSC is not as sensitive as DMTA in determining the T_g of a blend.[19]

The thermorheological complexity on chain dynamics and rheological behavior in miscible[20] polymer blends has been investigated.[6,21−27] According to Zawada et al.,[24] the monomeric friction coefficient of a miscible binary blend ($\zeta_{o,i}^{(b)}$) varies with blend composition in such a very complicated manner that at present there is no general rule which enables one to predict the viscosities of binary blends even when the monomeric friction coefficients of the constituent components ($\zeta_{o,i}^{(h)}$) are known.

In the past, the miscibility of PS/poly(α-methylstyrene) (PαMS) blends has been studied extensively.[28−33] In determining the miscibility of PS/PαMS blends, some research groups[28−31] used DSC to measure T_g, and another[33] measured cloud points to determine the critical temperature or binodal curve. Particularly noteworthy is an observation that the miscibility window of PS/PαMS blends is very sensitive to the type of solvent used in preparing the blends and the molecular weights of the constituent components.[29] Using DSC Lau et al.[28] observed a symmetric broadening of single glass transition in some PS/PαMS blends and attributed the observation to composition fluctuations near the critical point. Specifically, for blends consisting of PS having molecular weight (M_w) of 3.7×10^4 and PαMS having $M_w = 9.0 \times 10^4$, Lau et al.[28] observed that the breadth of glass transition, $\Delta T_g = T_{gf} - T_{gi}$, where T_{gi} denotes the onset point of glass transition and T_{gf} denotes the final point of glass transition, spanned 77 °C for a 25/75 PS/PαMS blend. However, very little, if any, has been reported on the rheological behavior of PS/PαMS blends.

Also, PS/PVME blends have received considerable attention from polymer scientists. Various aspects of the PS/PVME blend system have been investigated, namely, (a) phase equilibria,[34−36] (b) phase separation morphology,[34,36,37] (c) the kinetics of phase separation,[38,39] (d) the dependence of the Flory−Huggins interaction parameter on temperature and composition,[40,41] and (e) rheological behavior.[12−16] It is well-established that miscibility windows for the PS/PVME blend system are known to depend, among other factors, strongly on the molecular weight of the constituent components.

Very recently, we investigated the phase behavior and rheology of PS/PαMS and PS/PVME blend systems.

10.1021/ma980623l CCC: $15.00
Published on Web 11/07/1998

Table 1. Molecular Characteristics of PS and PαMS Synthesized in This Study

sample code	M_w (GPC)	M_w (LS)	M_w/M_n (GPC)
PS-38	38 700		1.04
PS-40	40 500		1.05
PS-58	58 700		1.03
PS-110	117 000		1.06
PαMS-18	18 000	20 200	1.04
PαMS-39	39 000	44 600	1.04
PαMS-47	47 400		1.04
PαMS-48	48 000	51 400	1.05

The present study was motivated largely by the desire to relate the rheological behavior of PS/PαMS or PS/PVME blends to their state of miscibility. For the study, the miscibility of PS/PαMS and PS/PVME blend systems, respectively, was investigated by T_g measurements via DSC and cloud point measurements via optical microscopy or light scattering, and the rheological behavior was investigated by oscillatory shear rheometry. In this paper we report the highlights of our findings.

Experimental Section

Materials. In this study, four PSs and four PαMSs were synthesized via anionic polymerization using an inert gas, stirred-tank reactor system.[42] In the polymerization of PS, cyclohexane was used as the solvent and the polymerization temperature was 35 °C, while, in the polymerization of PαMS, tetrahydrofuran was used as the solvent and the polymerization temperature was −78 °C. In both polymerizations, *sec*-butyllithium was used as the initiator. The molecular weights and molecular weight distributions of the PSs and PαMSs synthesized were determined by gel permeation chromatography (GPC) after constructing calibration curves for PS and PαMS, respectively, using 10 monodisperse PS standards (Scientific Polymer Products, Inc.) having M_w ranging from 2×10^3 to 2×10^6 and four monodisperse PαMS standards (Polyscience Co.), having M_w ranging from 10^4 to 4×10^5. Also employed was low-angle laser light scattering to determine the M_w of the PαMSs synthesized. For each PαMS, at least four different concentrations in toluene were prepared to determine M_w. Note that 0.124 mL/g was taken to be the specific refractive index increments (dn/dc) of PαMS in toluene at a wavelength of 632.8 nm.[43] The molecular characteristics of these polymers are summarized in Table 1. PVME in aqueous solution (50 wt %) was purchased from Aldrich Chemical Co. After completely removing the water, PVME was dissolved into toluene (5 wt % of solid) and precipitated using hexane. The M_w of PVME was determined, via low-angle laser light scattering, to be 9.43×10^4 using the value of $dn/dc = 0.063$ mL/g, and its molecular weight distribution (M_w/M_n) was determined, via GPC, to be 1.82 using the calibration curve of PS standards.

Sample Preparation. Four PS/PαMS blend systems were prepared: (1) PS-40/PαMS-18, (2) PS-38/PαMS-39, (3) PS-40/PαMS-48, each having various blend compositions (80/20, 60/40, 50/50, 40/60, and 20/80 by weight), and (4) 50/50 PS-58/PαMS-47 blend. PS/PαMS blend samples were prepared by dissolving a predetermined amount of the constituent components in benzene (10 wt % solids in solution) in the presence of 0.1 wt % antioxidant (Irganox 1010, Ciba-Geigy Group). The solution was freeze-dried at room temperature for 3 days under vacuum and further dried at 100 °C for 2 days under vacuum. The dried sample was compression molded at 175 °C for homopolymer PS and all PS/PαMS blends and at 185 °C for homopolymer PαMS into a sheet of 1 mm in thickness. Two additional blend specimens having compositions of 30/70 PS-110/PVME-95 and 50/50 PS-110/PVME-95, respectively, were prepared using a similar procedure. First, the benzene solution was freeze-dried at room temperature for 3 days under vacuum and then further dried at $T_g + 40$ °C for 2 days under vacuum. The dried sample was compression molded at $T_g + 70$ °C into a sheet having the thickness of approximately 1 mm.

Differential Scanning Calorimetry. The T_g of each blend specimen was measured using differential scanning calorimetry (Perkin-Elmer DSC 7 series). Prior to measurement, the base line was established using two empty pans. To prevent thermal degradation, nitrogen gas was circulated around the sample pan. For PS-40/PαMS-18, PS-38/PαMS-39, and PS-40/PαMS-48 blends, each specimen of approximately 15 mg was first heated to 230 °C at a heating rate of 20 °C/min, annealed there for 3 min, and then quenched to room temperature at a cooling rate of 200 °C/min. For PS-110/PVME-95 blends, each sample of approximately 15 mg was heated to $T_g + 50$ °C at a heating rate of 20 °C/min, annealed there for 3 min, and then quenched to $T_g - 50$ °C at a cooling rate of 200 °C/min. The second heating at a rate of 20 °C/min was used to determine the T_g of each specimen.

Cloud Point Determination. Eight blend compositions of PS-58/PαMS-47 were formed into films with thicknesses of approximately 100 μm, which were prepared by dissolving a predetermined amount of polymer into benzene (10 wt % in solid) in a Petri dish and evaporating solvent slowly for 8 h at room temperature in a fume hood. The last traces of solvent were completely removed using a vacuum oven at room temperature for 24 h and then at 140 °C for 24 h. The cloud points (T_b) of PS-58/PαMS-47 blends were determined by optical microscopy (Axioplan, Zeiss Co.) with a heating block where nitrogen gas was circulated. The T_b of a specimen was determined by the threshold temperature below which phase-separated structures were clearly seen under the optical microscope with a magnification of about 400× as the temperature was decreased gradually from the one-phase region (e.g., 220 °C for a 50/50 blend composition). It should be mentioned that before beginning optical microscopy, each specimen was annealed for 2 h at a preset temperature. Near the T_b of a specimen, the temperature inside the heating block was decreased stepwise with an interval of 1 °C; thus the maximum error in the values of T_b determined would be less than ±1 °C. For illustration, the morphology of a 50/50 PS-58/PαMS-47 blend annealed at 189 °C for 2 h is given in Figure 1a, and the morphology of a 50/50 PS-58/PαMS-47 blend annealed at 188 °C for 2 h is given in Figure 1b. At the magnification employed in Figure 1, we cannot observe evidence of phase separation at 189 °C, whereas we observe a co-continuous morphology, resulting from spinodal decomposition, at 188 °C. We then determined the T_b of this blend to be 188 °C. It should be mentioned that in determining the T_b of a PS-58/PαMS-47 blend specimen, we used optical microscopy instead of light scattering because, owing to a small difference in reflectivity index between PS and PαMS, light scattering was found to be *not* as effective as optical microscopy. On the other hand, the cloud points of PS-110/PVME-95 blends were determined using light scattering. Eight compositions of the PS-110/PVME-95 blend were prepared by dissolving a predetermined amount of polymer into toluene (10 wt % in solid) and evaporating the solvent slowly for 8 h at room temperature in a fume hood. The solvent was completely removed under vacuum at $T_g + 50$ °C for 24 h. The specimen thickness was about 15 μm, and the T_b was determined by the temperature at which the scattering intensity at the scattering angle of 30° increased abruptly during heating at a rate of 1 °C/h.

Rheological Measurement. Dynamic storage and loss moduli (G' and G'') were measured as functions of angular frequency (ω) ranging from 0.1 to 100 rad/s, at various temperatures during heating, using a Rheometrics Dynamic Spectrometer (Model RDS-II) in the oscillatory mode with parallel plate fixtures (25 mm diameter). Also, an Advanced Rheometrics Expanded System (ARES) was employed to measure G' and G'' as functions of ω ranging from 0.01 to 100 rad/s for PS-58/PαMS-47 and PS-110/PVME-95 blends. The measurement temperature was varied depending on the T_g of the specimen. The temperature control was accurate to within ±1 °C, and a fixed strain of 0.05 was used to ensure that

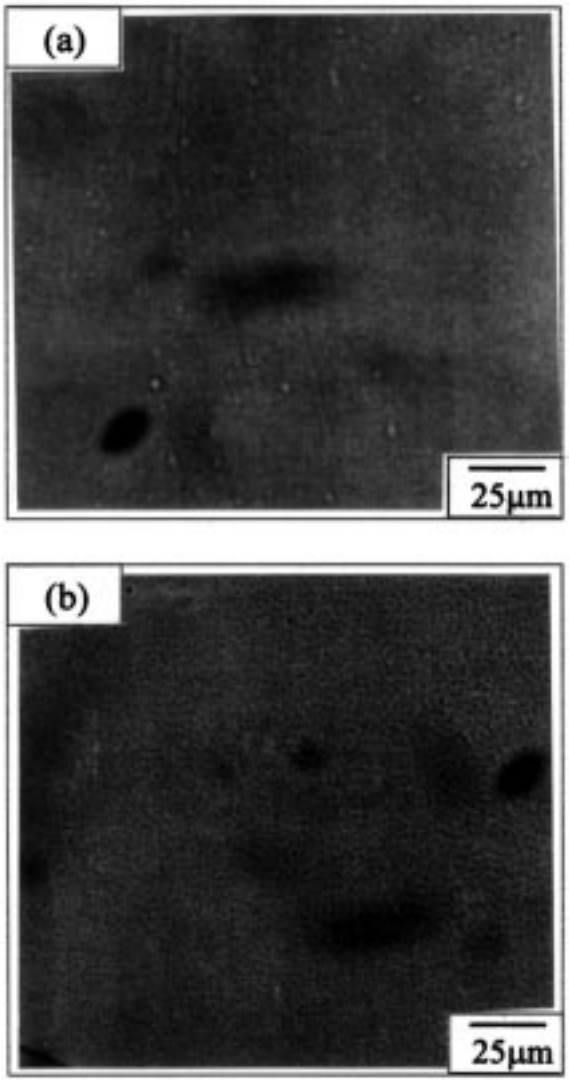

Figure 1. Optical micrographs of 50/50 PS-58/PαMS-47 blend specimens annealed at two different temperatures: (a) 189 °C for 2 h, and (b) 188 °C for 2 h.

measurements were taken well within the linear viscoelastic range of the materials investigated. All the rheological measurements were conducted under a nitrogen atmosphere in order to avoid oxidative degradation of the samples. For PS-40/PαMS-18, PS-38/PαMS-39, and PS-40/PαMS-48 blends, only one specimen was used for the entire range of ω at temperatures below 220 °C, while at higher temperatures a fresh specimen was used for each temperature. Since the experiment was conducted under a nitrogen atmosphere and one frequency sweep experiment lasted less than 25 min, thermal and/or oxidative degradation, if any, of the specimen is believed to be minimal.[42] This was confirmed later by the measurement via GPC of the molecular weight of the specimen before and after each rheological measurement. For PS-110/PVME-95 blends, only one specimen was used for the entire range of temperatures tested. In the phase-separated regime, rheological measurements were taken after a specimen was annealed for 1 h at a preset temperature.

Results

Glass Transition in PS/PαMS Blends. DSC traces for PS-38/PαMS-39 blends are given in Figure 2, showing a very broad, single glass transition for each blend composition, where the arrow upward denotes the onset point (T_{gi}), the symbol + denotes the midpoint (T_{gm}), and the arrow downward denotes the final point (T_{gf})

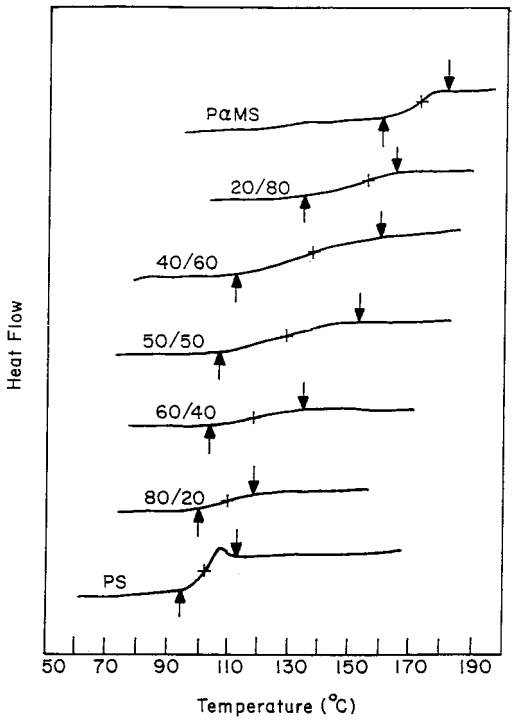

Figure 2. DSC traces for PS-38/PαMS-39 blends during heating at a rate of 20 °C/min, where the arrow pointing upward represents an onset point of glass transition T_{gi}, the arrow pointing downward represents the temperature at which glass transition is completed T_{gf}, and the symbol + represents the midpoint of glass transition T_{gm}.

Table 2. Summary of the Glass Transition Temperatures for the Three PS/PαMS Blend Systems Investigated in This Study

sample code	T_{gi} (°C)	T_{gm} (°C)	T_{gf} (°C)	ΔT_g (°C)
(a) PS-40/PαMS-18 Blend System				
PS-40	96	105	114	18
80/20 PS-40/PαMS-18	101	112	125	24
60/40 PS-40/PαMS-18	107	122	139	32
50/50 PS-40/PαMS-18	113	131	148	35
40/60 PS-40/PαMS-18	115	137	159	44
20/80 PS-40/PαMS-18	136	153	170	34
PαMS-18	161	173	185	24
(b) PS-38/PαMS-39 Blend System				
PS-38	95	103	113	18
80/20 PS-38/PαMS-39	98	108	117	19
60/40 PS-38/PαMS-39	103	117	134	31
50/50 PS-38/PαMS-39	105	127	151	46
40/60 PS-38/PαMS-39	112	137	159	45
20/80 PS-38/PαMS-39	132	153	163	31
PαMS-39	159	168	178	19
(c) PS-40/PαMS-48 Blend System				
PS-40	96	105	114	18
80/20 PS-40/PαMS-48	101	110	122	21
60/40 PS-40/PαMS-48	102	120	146	44
50/50 PS-40/PαMS-48	105	134	163	58
40/60 PS-40/PαMS-48	111	142	168	57
20/80 PS-40/PαMS-48	137	157	171	34
PαMS-48	169	177	189	20

of the glass transition. It seems reasonable to infer from Figure 2 that PS-38/PαMS-39 blends are miscible over the entire blend composition *if* a single glass transition is regarded as being necessary and sufficient conditions for miscibility. Similar results, though not shown here, were obtained for PS-40/PαMS-18 and PS-40/PαMS-48 blends. Table 2 gives a summary of the values of T_{gi}, T_{gm}, and T_{gf}, determined from DSC at a heating rate of 20 °C/min, of the three PS/PαMS blend systems inves-

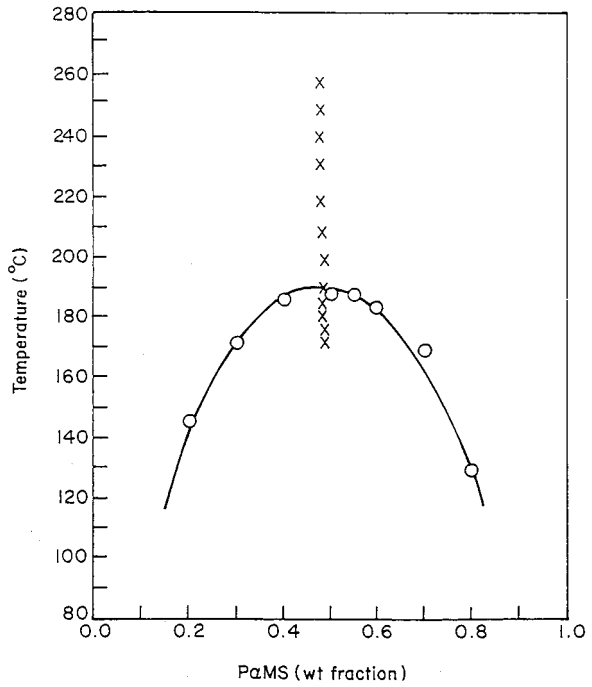

Figure 3. Composition-dependent cloud points (○) for PS-58/PαMS-47 blends determined from optical microscopy and the solid line (—) is a binodal curve calculated from curve-fitting experimental data to the Flory–Huggins theory. The symbol × denotes temperatures at which oscillatory shear experiments were conducted.

tigated in this study. Notice in Table 2 that the width of glass transition, $\Delta T_g = T_{gi} - T_{gf}$, is very large for some blend compositions. Earlier, Lin and Roe[31] also reported similarly large values of ΔT_g for PS/PαMS blend systems.

We found that during heating at 20 °C/min, a 50/50 PS-58/PαMS-47 blend undergoes two glass transitions, one at 107 °C slightly higher than the T_g of PS-58 and the other at 163 °C which is slightly lower than the T_g (170 °C) of PαMS-47. This observation is attributable to the phase separation which took place during heating at 20 °C/min although the specimen was annealed at 230 °C (above UCST) for 2 h followed by a rapid quenching to room temperature. Apparently, the heating rate employed during DSC was not fast enough to prevent phase separation. When a specimen was cooled at a rate of 20 °C/min from 230 °C to room temperature, we observed two glass transitions, one at 100 °C corresponding to the T_g of PS-58 and the other at 155 °C. This observation is consistent with the results of ref 31, reporting that when cooling was performed from a temperature in the homogeneous state to room temperature, two glass transitions were observed for a PS/PαMS blend until the cooling rate was very fast, say about 80 °C/min.

Phase Behavior and Rheology of PS-58/PαMS-47 Blends. Using optical microscopy, we determined cloud points for the PS-58/PαMS-47 blend system, the results (the symbol ○) of which are given in Figure 3. It should be mentioned that we could not determine cloud points for PS-40/PαMS-18, PS-38/PαMS-39, and PS-40/PαMS-48 blend systems, because the specimens were transparent over the entire blend composition within the highest experimental temperature employed, 230 °C. Using the cloud point measurements for the PS-58/PαMS-47 blend system, we obtained, with the aid of the Flory–Huggins theory, the following expression for the interaction parameter α:

$$\alpha = -2.165 \times 10^{-5} + (0.029 - 0.0021\phi_{P\alpha MS})/T \quad (1)$$

where α has units of mol/cm^3, $\phi_{P\alpha MS}$ is the volume fraction of PαMS, and T is the absolute temperature. We calculated the Flory–Huggins interaction parameter χ using the relationship $\chi = \alpha V_{ref}$ with V_{ref} being the reference volume, and the α-methylstyrene monomer was taken as a reference component. Also given in Figure 3 is the binodal curve (the solid line) calculated from the Flory–Huggins theory with the aid of eq 1. In calculating the binodal curve, we used the following expressions for the specific volume (in units of cm^3/g),

$$v_{PS} = 0.9199 + 5.098 \times 10^{-4}(T - 273) + 2.354 \times 10^{-7}(T - 273)^2 + [32.46 + 0.1017(T - 273)]/M_{w,PS} \quad (2)$$

for PS[44] in which $M_{w,PS}$ is the molecular weight of PS and

$$v_{P\alpha MS} = 0.87 + 5.08 \times 10^{-4}(T - 273) \quad (3)$$

for PαMS.[45] It can be seen in Figure 3 that the PS-58/PαMS-47 blend system exhibits UCST at 188 ± 1 °C and the critical weight fraction of PαMS is 0.5.

Earlier, Lin and Roe[33] obtained via light scattering the following expression for the interaction energy density Λ for PS/PαMS blend system

$$\Lambda = -5.6 \times 10^{-5}T + 0.0608 + 0.0018\phi_{P\alpha MS} \quad (4)$$

where Λ has units of cal/cm^3 and R is the universal gas constant. Since Λ is related to α by $\Lambda = \alpha RT$, eq 1 is consistent with eq 4 within experimental uncertainties. Note that eq 1 was obtained from optical microscopy and eq 4 from light scattering. It should be mentioned that although the third term in eq 4 has a sign opposite to the third term in eq 1, this does not affect much the values of α calculated from either eq 1 or eq 4, because the contribution of this term is quite small (say less than 10%) compared to that of the second term.

We conducted oscillatory shear flow measurements for a 50/50 PS-58/PαMS-47 blend at temperatures ranging from 170 to 260 °C, including the region below and above the binodal curve having UCST at 188 ± 1 °C. The temperatures at which rheological measurements were taken are indicated by the symbol × in Figure 3. Figure 4 gives plots of log G' versus log G'' for the 50/50 PS-58/PαMS-47 blend at various temperatures ranging from 170 to 260 °C. Following Neumann et al.,[46] hereafter log G' versus log G'' plots will be referred to as Han plots.[47] It can be seen in Figure 4 that Han plots depend on temperature from 170 °C in the two-phase region to 260 °C in the single-phase region; i.e., Han plots depend on temperatures in the miscible region, as determined from cloud point measurements, at temperatures as far away as approximately 70 °C above the UCST (188 ± 1 °C) of the PS-58/PαMS-47 blend system.

Since the specimens for the oscillatory shear experiments were prepared by compression molding followed by a rapid cooling from the molten state, we thought that there might be a possibility that the specimens had a kinetically frozen, phase-separated morphology. To

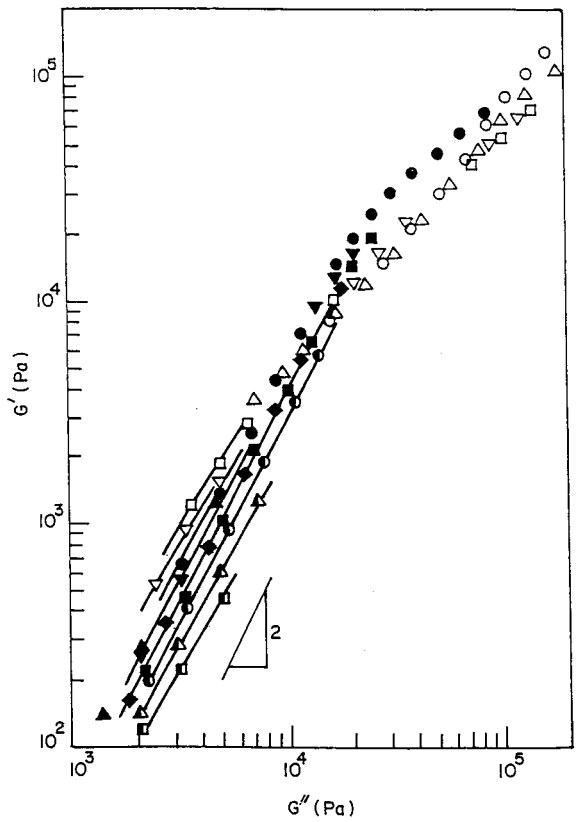

Figure 4. Han plots for a 50/50 PS-58/PαMS-47 blend at 170 (○), 175 (△), 180 (□), 185 (▽), 190 (●), 200 (▲), 210 (■), 220 (▼), 230 (◆), 240 (◐), 250 (◭), and 260 °C (◧).

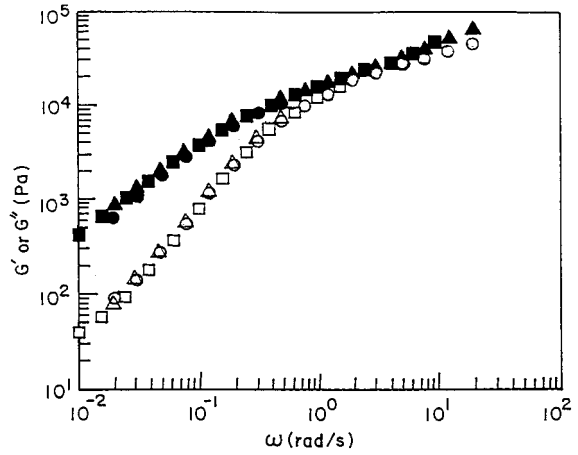

Figure 5. Plots of log G' versus log ω (open symbols) and log G'' versus log ω (filled symbols) for a 50/50 PS-58/PαMS-47 blend at 200 °C, which were obtained from repeated experiments at preset time intervals: (○, ●) the initial measurement, (△, ▲) the second measurement after resting for 1 h, and (□, ■) the third measurement after resting for 2 h.

check whether such a possibility existed or not, we repeated the frequency sweep experiment three times at a preset time interval for a 50/50 PS-58/PαMS-47 blend specimen after being heated to 200 °C, 12 °C above the UCST. Figure 5 gives the results of the frequency sweep experiments for the 50/50 PS-58/PαMS-47 blend specimen performed (i) right after the specimen was heated to 200 °C (the symbols ○ and ●), (ii) 1 h after the specimen was heated to 200 °C (the symbols △ and ▲), and (iii) 2 h after the specimen was heated to 200 °C (the symbols □ and ■). In Figure 5 we observe that log G' versus log ω and log G'' versus log ω plots for the three separate experiments overlap, leading us to conclude that the temperature dependence of Han plots observed in Figure 4 cannot be attributed to a possibility of having had kinetically frozen, phase-separated morphology in the specimens.

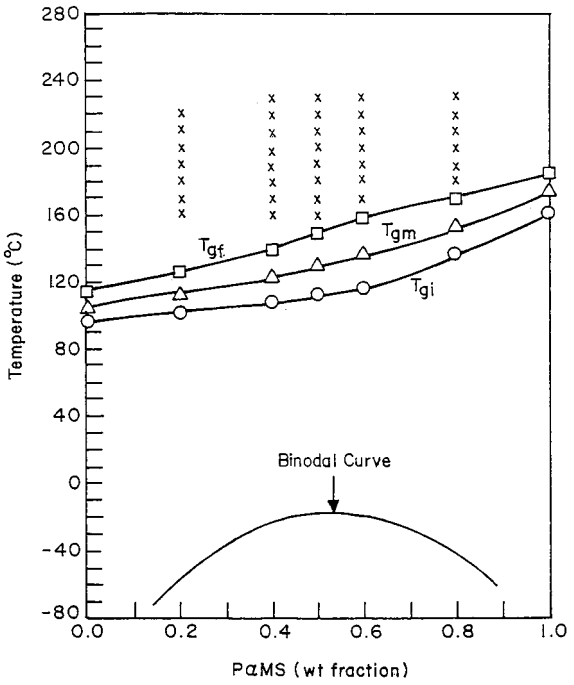

Figure 6. Composition-dependent glass transition temperatures T_{gi} (○), T_{gm} (△), and T_{gf} (□) for the PS-40/PαMS-18 blend system, binodal curve (—) calculated from the Flory−Huggins theory, and temperatures (the symbol ×) at which oscillatory shear experiments were conducted.

Phase Behavior and Rheology of the PS-40/PαMS-18 Blend System. Figure 6 gives composition-dependent T_{gi}, T_{gm}, and T_{gf} curves, and the temperatures (the symbol ×) at which rheological measurements were taken for the PS-40/PαMS-18 blend system. Also given in Figure 6 is the calculated binodal curve using eqs 1−3. Owing to the transparency of specimens, using optical microscopy, we could not determine cloud points for PS-40/PαMS-18 blends. It is interesting to observe that the calculated binodal curve lies far below the composition-dependent T_{gi} curve.

Figure 7 gives Han plots for a 50/50 PS-40/PαMS-18 blend, showing temperature independence and a slope of 2 in the terminal region at temperatures ranging from 160 to 210 °C. Similar observations, though not shown here, were also made for 80/20, 40/60, 60/40, and 20/80 PS-40/PαMS-18 blends. According to the rheological criterion by Han et al.,[49,52,53] we can conclude that PS-40/PαMS-18 blends form a homogeneous phase over the entire range of blend compositions investigated. The above conclusion can readily be understood when the readers are reminded that the calculated binodal curve for the PS-40/PαMS-18 blend system lies very far below the composition-dependent T_{gi} curve (see Figure 6).

Phase Behavior and Rheology of the PS-38/PαMS-39 Blend System. Figure 8 gives composition-dependent T_{gi}, T_{gm}, and T_{gf} curves and the temperatures (the symbol ×) at which rheological measurements were taken for the PS-38/PαMS-39 blend system. Also given in Figure 8 is the calculated binodal curve using eqs 1−3. Owing to the transparency of specimens, using optical microscopy, we could not determine cloud points for PS-38/PαMS-39 blends. It is interesting to observe

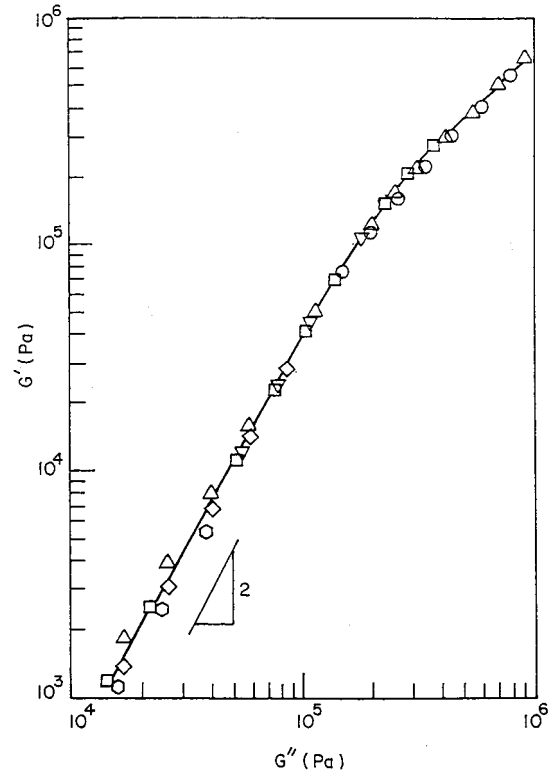

Figure 7. Han plots for the 50/50 PS-40/PαMS-18 blend at 160 (○), 170 (△), 180 (□), 190 (▽), 200 (◇), and 210 °C (⬡).

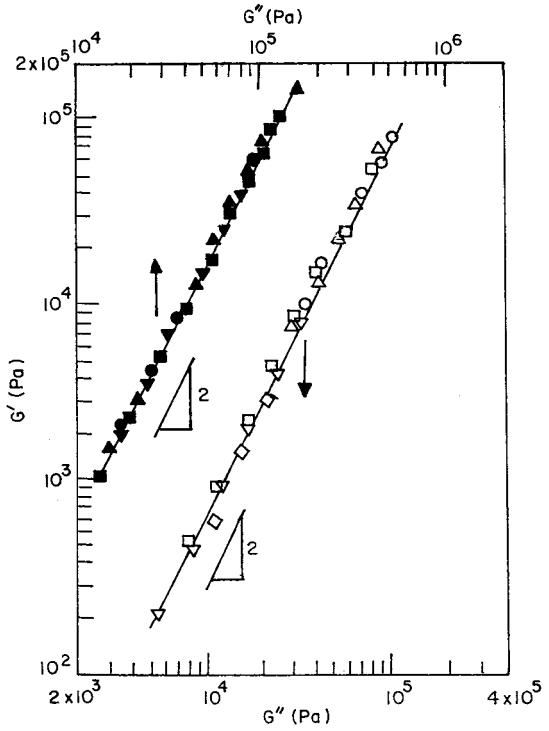

Figure 9. Han plots (a) for the 80/20 PS-38/PαMS-39 blend at 160 (○), 170 (△), 180 (□), 190 (▽), and 200 °C (◇) and (b) for the 20/80 PS-38/PαMS-39 blend at 200 (●), 210 (▲), 220 (■), and 230 °C (▼).

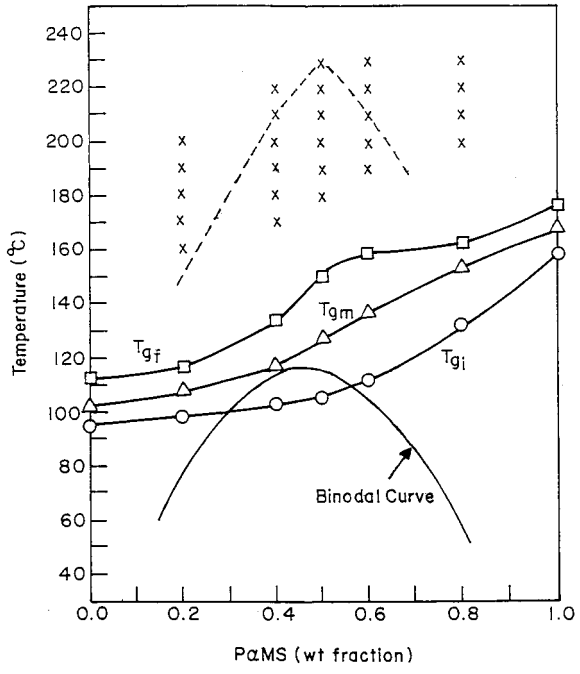

Figure 8. Composition-dependent glass transition temperatures T_{gi} (○), T_{gm} (△), and T_{gf} (□) for the PS-38/PαMS-39 blend system, binodal curve (—) calculated from the Flory−Huggins theory, and temperatures (the symbol ×) at which oscillatory shear experiments were conducted.

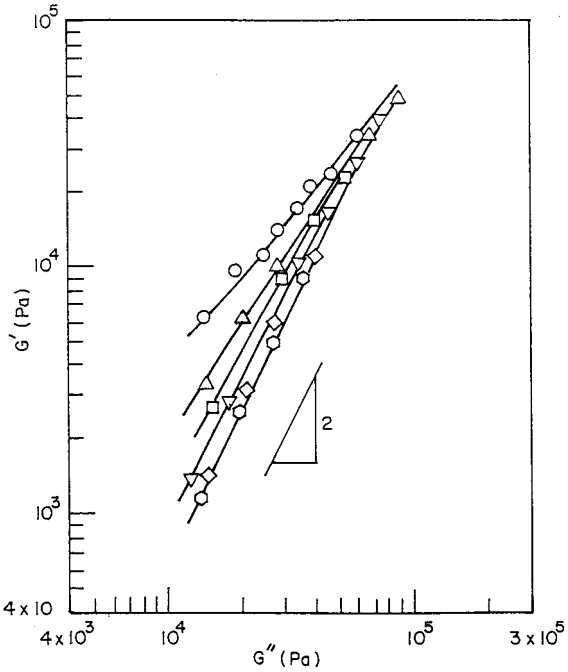

Figure 10. Han plots for the 60/40 PS-38/PαMS-39 blend at 170 (○), 180 (△), 190 (□), 200 (▽), 210 (◇), and 220 °C (⬡).

that the calculated binodal curve lies between the composition-dependent T_{gi} and T_{gm} curves.

Figure 9 gives Han plots for 80/20 and 20/80 PS-38/PαMS-39 blends, showing temperature independence and a slope of 2 in the terminal region over the range of temperatures investigated. Thus, we can conclude that the 80/20 and 20/80 PS-38/PαMS-39 blends are miscible. Figure 10 gives Han plots for a 60/40 PS-38/PαMS-39blend at temperatures ranging from 170 to 220 °C. It is of interest to observe in Figure 10 that Han plots at temperatures from 170 to 210 °C show temperature dependence which, however, diminishes as the temperature is increased further to 220 °C, and the slope of Han plots increases gradually from much less than 2 at 170 °C toward 2 as the temperature is increased to 210 and 220 °C. We made a similar observation for the 50/50 PS-38/PαMS-39 blend in that Han plots exhibited temperature dependence up to 220

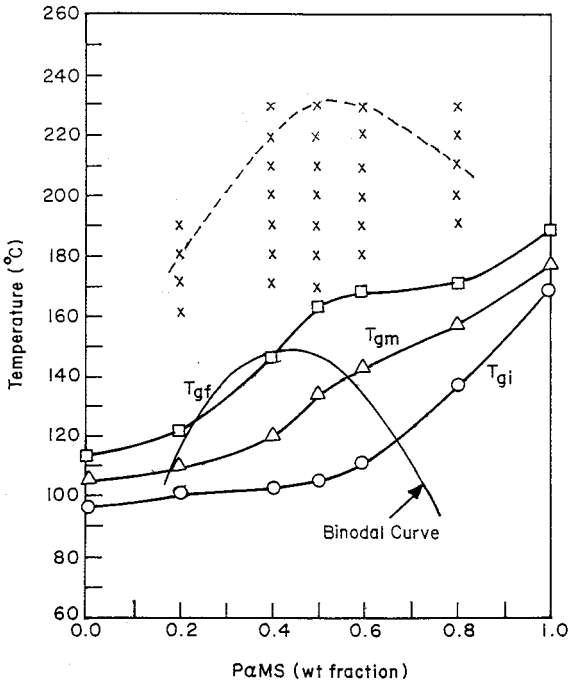

Figure 11. Composition-dependent glass transition temperatures T_{gi} (○), T_{gm} (△), and T_{gf} (□) for the PS-40/PαMS-48 blend system, binodal curve (—) calculated from the Flory−Huggins theory, and temperatures (the symbol ×) at which oscillatory shear experiments were conducted.

°C and then temperature independence as the temperature was increased from 220 to 230 °C.

Phase Behavior and Rheology of the PS-40/PαMS-48 Blend System. Figure 11 gives composition-dependent T_{gi}, T_{gm}, and T_{gf} curves and the temperatures (the symbol ×) at which rheological measurements were taken for the PS-40/PαMS-48 blend system. Also given in Figure 11 is the calculated binodal curve using eqs 1−3. Owing to the transparency of specimens, using optical microscopy we could not determine cloud points for PS-40/PαMS-48 blends. It is interesting to observe that the calculated binodal curve lies slightly above the composition-dependent T_{gf} curve.

Figure 12 gives Han plots for a 80/20 PS-40/PαMS-48 blend, showing temperature dependence at temperatures ranging from 160 to 180 °C, which, however, diminishes as the temperature is increased further to 190 °C. Although not shown here due to space limitation, we found that Han plots for a 20/80 PS-40/PαMS-48 blend show temperature dependence up to 220 °C and then temperature independence as the temperature is increased further to 230 °C. Figure 13 gives Han plots for a 50/50 PS-40/PαMS-48 blend at temperatures ranging from 170 to 230 °C, in which we observe that Han plots in the terminal region show temperature dependence up to the highest experimental temperature employed, 230 °C.

Glass Transition, Phase Behavior, and Rheology of the PS-110/PVME-95 Blend System. DSC traces for PS-110/PVME-95 blends are given in Figure 14, showing a very broad, single glass transition for each blend composition, where the arrow upward denotes the onset point (T_{gi}), the symbol + denotes the midpoint (T_{gm}), and the arrow downward denotes the final point (T_{gf}) of the glass transition. One may infer from Figure 14 that each PS-110/PVME-95 blend, when annealed below the LCST, exhibits a single glass transition. We

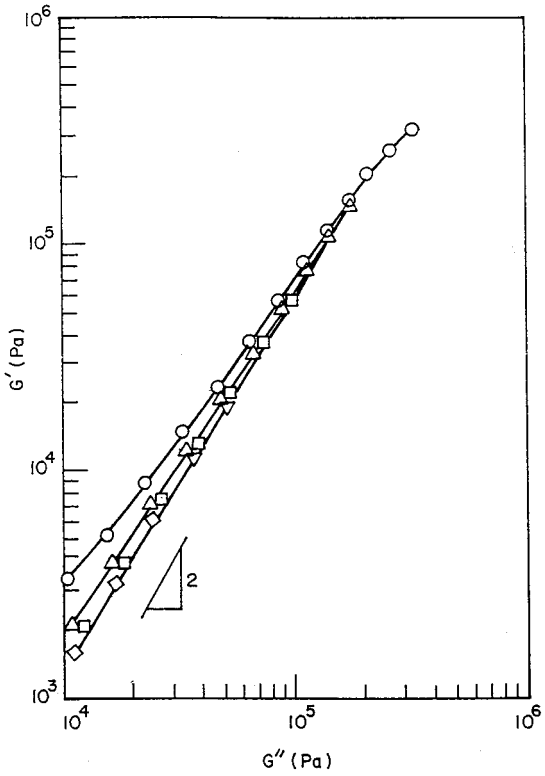

Figure 12. Han plots for the 80/20 PS-40/PαMS-48 blend at 160 (○), 170 (△), 180 (□), 190 (▽), and 200 °C (◇).

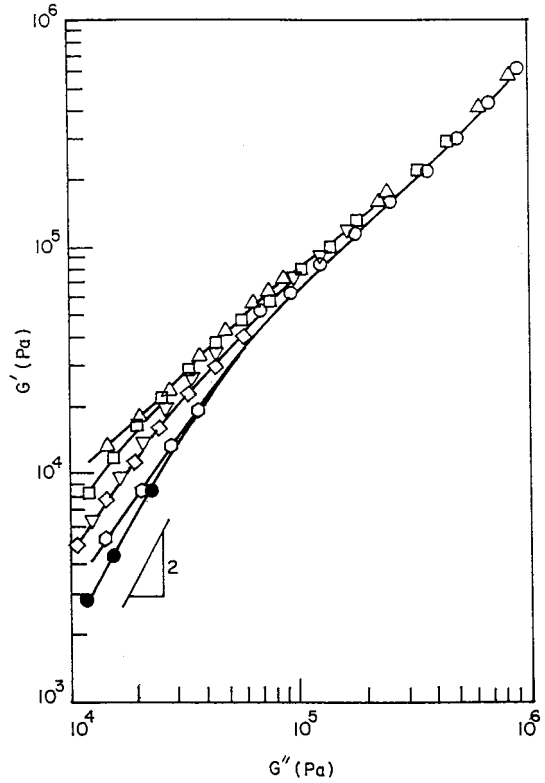

Figure 13. Han plots for the 50/50 PS-40/PαMS-48 blend at 170 (○), 180 (△), 190 (□), 200 (▽), 210 (◇), 220 (⬡), and 230 °C (●).

found, however, that each blend, when annealed above the LCST, exhibited two distinct T_gs. Specifically, we observed that the 30/70 PS-110/PVME-95 blend, when annealed at 140 °C for 1 h and quenched to −80 °C, exhibited two T_gs: one at −30 °C that represents the T_g of PVME and the other at 80 °C that represents the

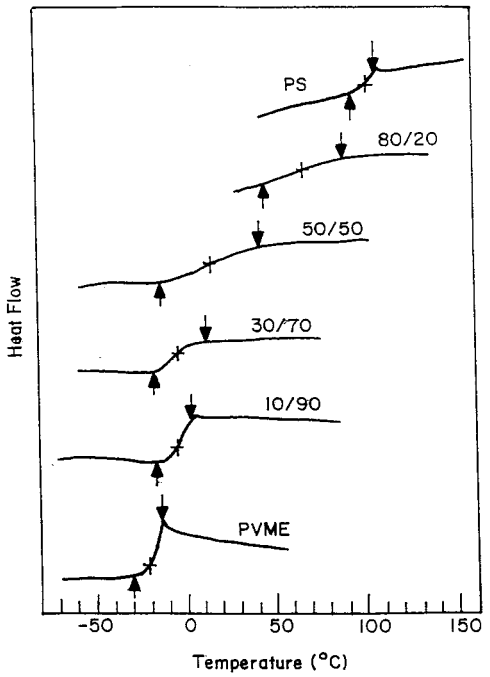

Figure 14. DSC traces for PS-110/PVME-95 blends during heating at a rate of 20 °C/min, where the arrow pointing upward represents an onset point of glass transition T_{gi}, the arrow pointing downward represents the temperature at which glass transition is completed T_{gf}, and the symbol + represents the midpoint of glass transition T_{gm}.

Table 3. Glass Transition Temperatures for the PS/PVME Blend System Investigated in This Study

sample code	T_{gi} (°C)	T_{gm} (°C)	T_{gf} (°C)	ΔT_g[a] (°C)
PS-110	97.7	102.5	107	9.3
80/20 PS-110PVME−95	48.3	65.0	83.0	34.7
50/50 PS-110PVME−95	−7.0	12.3	35.0	42.0
30/70 PS-110PVME−95	−17.5	−6.0	8.7	26.2
10/90 PS-110PVME−95	−23.5	−12.0	−2.5	21.0
PVME−95	−28.0	−18.0	−14.0	14.0

[a] $\Delta T_g = T_{gf} - T_{gi}$.

T_g of the PS-rich phase. Table 3 gives a summary of the values of T_{gi}, T_{gm}, and T_{gf} for the PS-110/PVME-95 blend system. Notice in Table 3 that $\Delta T_g = T_{gi} - T_{gf}$ is very large for some blend compositions. Earlier, similar results were reported by Schneider and Wirbser[15] for PS/PVME blends.

Figure 15 gives composition-dependent cloud points (the symbol ●), composition-dependent T_{gi}, T_{gm}, and T_{gf} curves, and the temperatures (the symbol ×) at which rheological measurements were taken for the PS-110/PVME-95 blend system. Using the cloud point measurements for the PS-110/PVME-95 blend system together with the Flory−Huggins theory, we obtained the following expression for α:

$$\alpha = 0.478 \times 10^{-3} - (0.176 + 0.0062\phi_{PS})/T \quad (5)$$

where ϕ_{PS} is the volume fraction of PS. The solid line in Figure 15 describes the binodal curve calculated from the Flory−Huggins theory with the aid of eq 5. In calculating the binodal curve we used the following expression for the specific volume (in units of cm^3/g):

$$v_{PVME} = 1/[1.0717 - 7.67 \times 10^{-4}(T - 273) + 2.8 \times 10^{-7}(T - 273)^2] \quad (6)$$

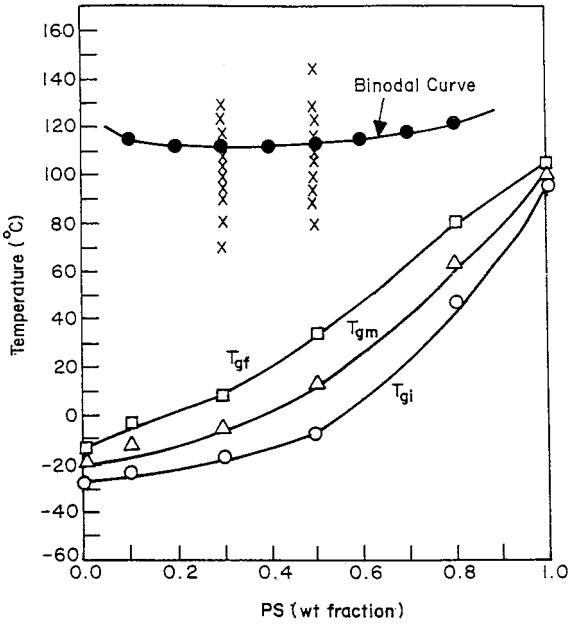

Figure 15. Composition-dependent cloud points (●) determined from light scattering and glass transition temperatures T_{gi} (○), T_{gm} (△), and T_{gf} (□) for PS-110/PVME-95 blends. The solid line (—) is a binodal curve calculated from curve-fitting experimental data to the Flory−Huggins theory. The symbol × denotes temperatures at which oscillatory shear experiments were conducted.

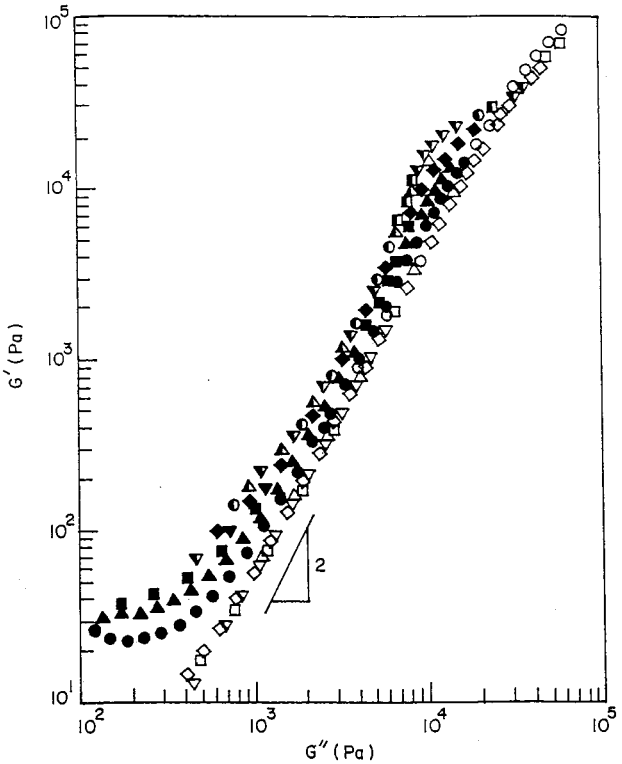

Figure 16. Han plots for the 30/70 PS-110/PVME-95 blend at 70 (○), 80 (△), 90 (□), 95 (▽), 100 (◇), 105 (●), 108 (▲), 110 (■), 112 (▼), 113 (♦), 117 (◐), 120 (◭), 125 (◧), and 130 °C (▼).

for PVME.[13] Note in Figure 15 that the binodal curve for the PS-110/PVME-95 blend system exhibits LCST at 112 ± 1 °C and the critical weight fraction of PS in the blend is 0.3.

Figure 16 gives Han plots for a 30/70 PS-110/PVME-95 blend at various temperatures ranging from 70 °C in the single-phase region to 130 °C in the two-phase

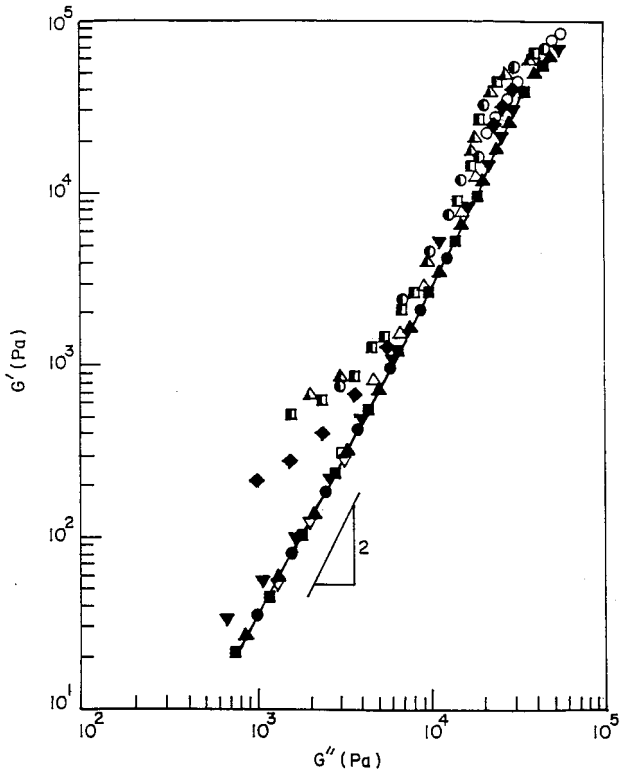

Figure 17. Han plots for the 50/50 PS-110/PVME-95 blend at 80 (○), 90 (△), 95 (□), 100 (▽), 105 (◇), 108 (●), 110 (▲), 112 (■), 114 (▼), 118 (◆), 130 (◐), 140 (◭), and 145 °C (◧).

region. In Figure 16 we observe that the Han plot has the slope of 2 in the terminal region at $T \leq 100$ °C and begins to exhibit temperature dependence at 105 °C, which is still in the single-phase region according to the phase diagram (see Figure 15). It can be seen in Figure 16 that Han plots depend on temperatures in the miscible region, as determined from cloud point measurements (see Figure 15), at temperatures as far away as approximately 7 °C below the LCST (112 ± 1 °C) of the PS-110/PVME-95 blend system. The value of 7 °C for the PS-110/PVME-95 blend system is quite small compared to the value of 70 °C observed above for the PS-58/PαMS-47 blend system (see Figure 4).

Figure 17 gives Han plots for a 50/50 PS-110/PVME-95 blend, which is an off-critical blend composition. In Figure 17 we observe that the Han plot in the terminal region has the slope of 2, exhibits temperature independence at $T \leq 112$ °C, and begins to show temperature dependence at 114 °C, which is the cloud point for the 50/50 PS-110/PVME-95 blend according to the phase diagram (see Figure 15). This observation is at variance from that made above for PS-38/PαMS-39 and PS-40/PαMS-48 blend systems (see Figures 10, 12, and 13).

The above observations are very similar to those reported by Ajji et al.[14] Very recently Kapnistos et al.[16] reported that Han plots for a 20/80 PS/PVME blend, which was the critical composition, showed a temperature dependence of 3−13 °C below LCST (93 °C), whereas Han plots for an off-critical composition (70/30 PS/PVME blend) did not show a temperature dependence. They ascribed the temperature dependence of Han plots of the critical composition (20/80 PS/PVME blend) to dynamical composition fluctuations (see Figure 10 in ref 16) near the LCST. Following the view of Kapnistos et al.,[16] we can conclude that the PS-110/PVME-95 blend system investigated in this study has

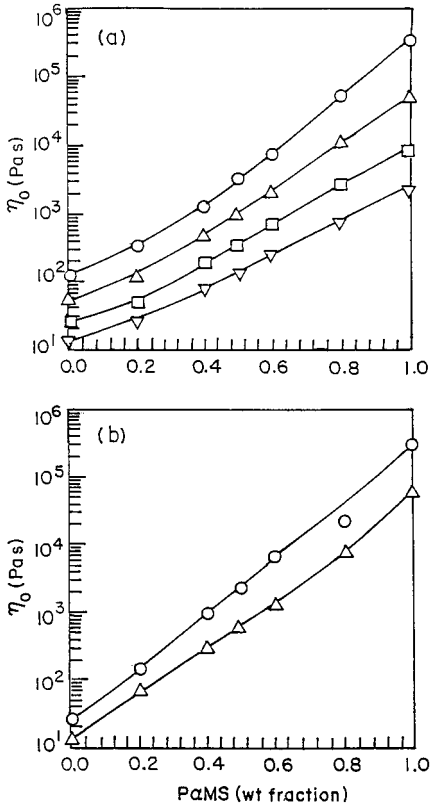

Figure 18. (a) Composition dependence of η_0 in the PS-40/PαMS-18 blend system at 190 (○), 200 (△), 210 (□), and 220 °C (▽). (b) Composition dependence of η_0 in the PS-40/PαMS-48 blend system at 200 (○) and 220 °C (△).

dynamical composition fluctuations of approximately 7 °C, which is in agreement with the observation made by Kapnistos et al.[16] It should be mentioned, however, that the PVMEs employed in the two studies have different values of M_w/M_n, namely, $M_w/M_n = 1.82$ for PVME-95 employed in the present study and $M_w/M_n = 1.35$ for the PVME employed in the study of Kapnistos et al.[16]

Composition Dependence of Zero-Shear Viscosity of PS/PαMS Blends. The composition dependence of zero-shear viscosity (η_0) is given in Figure 18a for the PS-40/PαMS-18 blend system at 190, 200, 210, and 220 °C and in Figure 18b for the PS-40/PαMS-48 blend system at 210 and 220 °C. In Figure 18 we observe that the composition dependence of η_0 under isothermal conditions shows *negative* deviations from linearity, very similar to the previous results reported in the literature.[3,4,8−11] We made a similar observation, though not shown here, for the PS-38/PαMS-39 blend system. On the other hand, the previous study[6] on binary blends consisting of 1,2- and 1,4-polybutadiene suggests that we should expect to observe *positive* deviations from linearity in the plots of log η_0 versus blend composition for PS/PαMS blends having very small values of χ (e.g., about 0.0044 at 190 °C). The discrepancy between Figure 18 and the previous study[6] may be due to the low molecular weights of PS and PαMS employed in this study. In such a situation, owing to the constraint release process taking place, the tube model or the reptation concept must be modified and thus the actual viscosity would be lower than the estimated value on the basis of the reptation model without constraint release.[51]

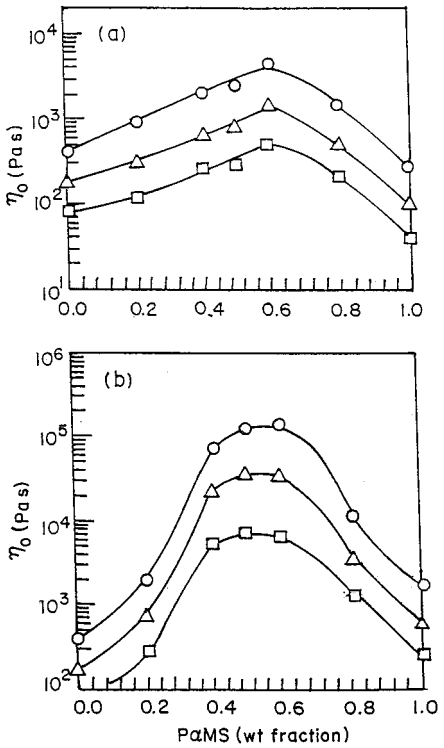

Figure 19. (a) Composition dependence of η_0 in the PS-40/PαMS-18 blend system at T_{gi} + 80 °C (○), T_{gi} + 90 °C (△), and T_{gi} + 100 °C (□). (b) Composition dependence of η_0 in the PS-40/PαMS-48 blend system at T_{gi} + 80 °C (○), T_{gi} + 90 °C (△), and T_{gi} + 100 °C (□).

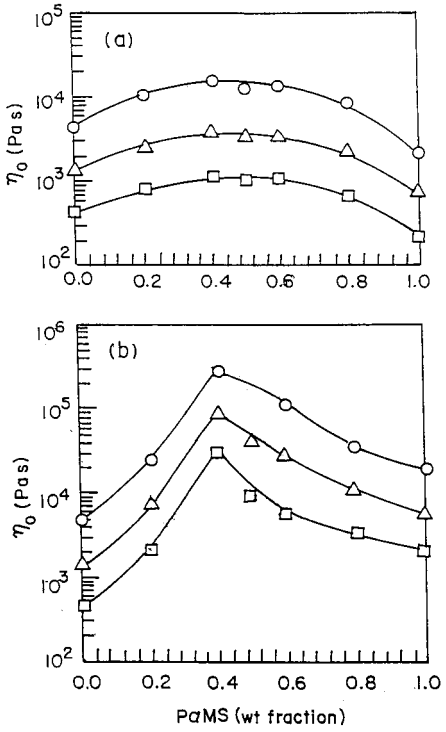

Figure 20. (a) Composition dependence of η_0 in the PS-40/PαMS-18 blend system at T_{gm} + 50 °C (○), T_{gm} + 60 °C (△), and T_{gm} + 70 °C (□). (b) Composition dependence of η_0 in the PS-40/PαMS-48 blend system at T_{gm} + 50 °C (□), T_{gm} + 60 °C (△), and T_{gm} + 70 °C (□).

Earlier, several research groups[7,21,25−27] suggested use of iso-free volume conditions (or at temperatures which are at an equal distance from the T_gs of the respective blend compositions), instead of isothermal conditions, in investigating composition dependence of η_0 of miscible polymer blends. However, a serious question may be raised as to which of the T_g values (i.e., T_{gi}, T_{gm}, or T_{gf}) should be used when the breadth of glass transition varies significantly with blend composition (see Tables 2 and 3).

The composition dependence of η_0 is given in Figure 19a for the PS-40/PαMS-18 blend system and in Figure 19b for the PS-40/PαMS-48 blend system, at T_{gi} + 80 °C, T_{gi} + 90 °C, and T_{gi} + 100 °C, respectively, where T_{gi} is used as a reference temperature. It is of interest to observe in Figure 19 that η_0 goes through a maximum at a certain blend composition, the extent of which is greater for the PS-40/PαMS-48 blend system than for the PS-40/PαMS-18 blend system. When using T_{gm} as a reference temperature, we observe a different composition dependence of η_0, as given in Figure 20a for the PS-40/PαMS-18 blend system and in Figure 20b for the PS-40/PαMS-48 blend system, at T_{gm} + 50 °C, T_{gm} + 60 °C, and T_{gm} + 70 °C, respectively. It is clear from Figures 19 and 20 that the composition dependence of η_0 looks quite different, depending on whether T_{gi} or T_{gm} is used as a reference temperature. We thus conclude that the dynamical behavior of chains in a PS/PαMS blend do not follow the average mobility of the blend at T_{gm}, in agreement with the conclusion drawn by Zawada et al.[23]

Discussion

Microheterogeneity in Miscible PS/PαMS and PS/PVME Blends. Earlier, the temperature dependence of the Han plot, similar to that in Figures 10, 12, and 13, was observed in microphase-separated block copolymers at temperatures below a certain critical temperature,[52] referred to as the order−disorder transition temperature, and in thermotropic liquid-crystalline polymers at temperatures below a certain critical temperature,[53] referred to as the isotropization (or clearing) temperature. It should be pointed out, however, that according to the rheological criteria established by Han et al.,[49,52,53] Han plots must not only be independent of temperature but also have a slope of 2 in the terminal region if a polymer is to be regarded as being truly homogeneous. That is, if both criteria are not met, a polymer cannot be regarded as being homogeneous. This observation can best be illustrated by the Han plots for poly(acrylonitrile-*stat*-butadiene-*stat*-styrene) (PABS),[49a] which show temperature independence but have a slope in the terminal region much less than 2. It is a well-established fact that PABS has polybutadiene rubber particles grafted on the matrix of poly(styrene-*stat*-acylonitrile) and thus PABS is a highly heterogeneous polymer. Since the rubber particles in PABS are grafted chemically on the matrix, the morphological state of PABS does not change with temperature, thus giving rise to a temperature-independent Han plot. But owing to the heterogeneity of PABS, the slope of the Han plot in the terminal region is much less than 2. In other words, the temperature independence alone of the Han plot is not sufficient for a polymer to be regarded as being homogeneous.

On the basis of the observations made above, we can conclude that (i) the 60/40 PS-38/PαMS-39 blend has microheterogeneity until the temperature is increased to about 210 °C (see Figure 10), (ii) the 80/20 PS-40/PαMS-48 blend has microheterogeneity until the temperature is increased to about 180 °C (see Figure 12),

and (iii) the 50/50 PS-40/PαMS-48 blend has microheterogeneity until the temperature is increased to about 230 °C (see Figure 13). The above conclusions suggest to us that composition-dependent microheterogeneity exists above the binodal curve, i.e., in the miscible region between the binodal curve and the dotted line in Figure 8 for the PS-38/PαMS-39 blend system and in Figure 11 for the PS-40/PαMS-48 blend system. Note in Figures 8 and 11 that the dotted line, having a shape very similar to that of the calculated binodal curve, is shifted upward about 80−100 °C above the calculated binodal curve of the respective blend systems. The readers are reminded that all three PS-40/PαMS-18, PS-38/PαMS-39, and PS-40/PαMS-48 blend systems are miscible, as judged by both DSC and optical microscopy, over the entire range of blend compositions. On the other hand, we observe from Figure 16 that microheterogeneity in PS/PVME blends exists within a much narrower range of temperatures (<7 °C). It is appropriate to mention at this juncture that a dynamic mechanical thermal analysis (DMTA) can resolve the size of domains (or separated phases) on the order of 5−10 nm[18] and DSC is not as sensitive as DMTA in determining the T_g of a blend.[19] This then suggests that DSC may not be able to detect the size of domains smaller than approximately 20 nm and optical microscopy (or light scattering) cannot detect the existence of domains smaller than approximately 500 nm. This observation seems to suggest that a very broad, single glass transition in a binary blend does not warrant that the blend is miscible on the segmental level.

Factors Controlling Dynamical Composition Fluctuations in Miscible PS/PαMS and PS/PVME Blends. In view of the fact that a binodal curve constructed from equilibrium thermodynamics (i.e., from the Flory−Huggins theory) determines the boundary between the homogeneous and inhomogeneous regions in a mixture of two liquids, we are led to conclude that the presence of microheterogeneity discussed above in both PS/PαMS and PS/PVME blend systems is attributable to dynamical composition fluctuations near the critical point. We now offer an explanation as to why the extent of dynamical composition fluctuations is much greater in PS/PαMS blends than in PS/PVME blends, as determined from a larger temperature dependence of Han plots in the miscible region of PS/PαMS blends than in the miscible region of PS/PVME blends.

The extent of concentration fluctuations, $\epsilon = 2[1 - (\chi/\chi_c)]$, of a polymer blend near its critical temperature can be expressed by

$$\epsilon \approx \frac{4(1-\phi_{2,c})\phi_{2,c}r_1r_2}{(1-\phi_{2,c})r_1+\phi_{2,c}r_2}\left(\frac{d\chi}{dT}\right)_c(T_c - T) \qquad (7)$$

where χ_c is the value of χ at the critical temperature T_c, $\phi_{2,c}$ is the critical volume fraction of the reference component (PαMS for PS/PαMS blends and PS for PS/PVME blends), and r_i ($i = 1, 2$) is the number of segments (or degree of polymerization) of component i. In obtaining eq 7, use was made of[54]

$$2\chi_c = \frac{1}{r_1\phi_{1,c}} + \frac{1}{r_2\phi_{2,c}} \qquad (8)$$

If we use the following expression for α,

$$\alpha = A + B/T + C\phi_2/T \qquad (9)$$

in eq 7, we obtain

$$\epsilon \approx \frac{4(1-\phi_{2,c})\phi_{2,c}r_1r_2}{(1-\phi_{2,c})r_1+\phi_{2,c}r_2}V_{ref}\left(\frac{B+C\phi_{2,c}}{T_c^{\,2}}\right)(T - T_c) \qquad (10)$$

in which use was made of $\chi = \alpha V_{ref}$ with V_{ref} being the molar volume of a reference component. A close look at eq 10 indicates that the coefficient B in eq 9 plays a predominant role in determining the extent of composition fluctuations, ϵ, near the critical point, because the magnitude of $C\phi_2$ is much smaller than that of B, as can be seen from eq 1 or eq 5.

It is appropriate to mention at this juncture that earlier Onuki[55] obtained an expression, similar to eq 7, for AB-type diblock copolymers. Subsequently, Han et al.[52c,d] used Onuki's expression to discuss the extent of composition fluctuations in polystyrene-*block*-polyisoprene-*block*-polystyrene and polystyrene-*block*-polyisoprene copolymers near the order−disorder transition temperature.

Substituting eq 1 for PS/PαMS blends and eq 5 for PS/PVME blends, respectively, into eq 10, we obtain the following relationship:

$$(T - T_c)_{PS/P\alpha MS} \approx 15(T_c - T)_{PS/PVME} \qquad (11)$$

for the same value of ϵ in both PS/PαMS and PS/PVME blend systems. Equation 11 suggests that the range of temperature over which dynamical composition fluctuations near the critical point may persist is approximately 15 times greater in PS/PαMS blends than in PS/PVME blends. This analysis now seems to explain, at least in part, our experimental results (compare Figure 4 for a 50/50 PS-58/PαMS-47 blend with Figure 16 for a 30/70 PS-110/PVME-95 blend).

Concluding Remarks

In this paper, on the basis of oscillatory shear rheometry we have shown that PS/PαMS blends exhibiting UCST have microheterogeneity in the miscible region (i.e., at temperatures above the binodal curve) and PS/PVME blends exhibiting LCST also have microheterogeneity in the miscible region (i.e., at temperatures below the binodal curve), where the miscibility region was determined by optical microscopy or light scattering. We attributed the presence of microheterogeneity in the respective blend systems investigated to dynamical composition fluctuations near the critical point. We offered an explanation as to why PS/PαMS blends exhibit much greater dynamical composition fluctuations than PS/PVME blends, in terms of the difference in temperature dependence of the interaction parameter between the two blend systems.

Previously, the presence of microhetrogeneity in miscible PS/PVME blends was conjectured by the observation of a very broad, single glass transition.[15] In this paper we have shown that a broad, single glass transition in a miscible polymer blend does not necessarily signify the presence of microheterogeneity. This is demonstrated clearly by the PS-40/PαMS-18 blend system investigated in this study in that we find no evidence of microheterogeneity in PS-40/PαMS-18 blends, as determined from oscillatory shear rheometry (see Figure 7), although the same blends exhibit a broad, single glass transition (see Figure 6). Thus we conclude

that Han plots are very effective in investigating whether or not microheterogeneity is present in a miscible polymer blend.

At this juncture, it is worth mentioning a recent study of Müller et al.[56] who, using an electron spin relaxation (ESR) technique, observed microheterogeneity on the segmental level (as small as 5 nm) in poly[styrene-*co*-(maleic anhydride)] (PSMA)/PVME blends, exhibiting LCST, at temperatures approximately 70 °C below the cloud point determined from light scattering. Note that light scattering cannot detect the size of phase-separated domains smaller than its wavelength, approximately 500 nm. According to Müller et al.,[56] a small amount of maleic anhydride groups (4.8 wt %) in the PSMA had a negligible effect on the phase behavior of PSMA/PVME blends, and thus PSMA/PVME blends can be regarded as being virtually the same as PS/PVME blends. The results of ESR by Müller et al.[56] support the findings of the present study (see Figure 16), suggesting that microheterogeneity, which was determined from a Han plot via oscillatory shear rheometry, is present in a 30/70 PS-110/PVME-95 blend. It would be a very challenging task to investigate the presence of microheterogeneity in PS/PαMS blends using sophisticated experimental techniques, such as ESR, solid-state nuclear magnetic resonance spectroscopy, or small-angle neutron scattering technique.

In this paper we have pointed out that any attempt to explain the dependence of zero-shear viscosity on blend composition of miscible polymer blends under iso-free volume conditions requires extreme care, because miscible blends undergoing a very broad, single glass transition will give different results, depending on which of the T_gs (T_{gi}, T_{gm}, or T_{gf}) is chosen.

Before closing, we wish to point out that the composition-dependent characteristic relaxation time for the PS/PαMS and PS/PVME blend systems investigated in this study could not be calculated, because these blends did not exhibit a maximum in log G'' versus log ω plots within the range of angular frequencies employed (100 rad/s was the highest experimentally accessible frequency). To observe a maximum in log G'' versus log ω plots, much higher molecular weights of PS and PαMS than those employed in this study would be required. But a very high molecular weight PS/PαMS or PS/PVME blend will become immiscible over the entire range of blend compositions. Thus we have concluded that both PS/PαMS and PS/PVME blend systems have a practical limitation which prevents us from having a maximum in log G'' versus log ω plots (thus composition-dependent characteristic relaxation time).

Acknowledgment. We wish to acknowledge that Professor Taehyun Chang kindly measured via low-angle laser light scattering the weight-average molecular weights of the three PαMSs and PVME employed in this study.

References and Notes

(1) Prest, W. M.; Porter, R. S. *J. Polym. Sci., A-2* **1972**, *10*, 1639.
(2) Chuang, H. K.; Han, C. D. *J. Appl. Polym. Sci.* **1984**, *29*, 2205.
(3) Han, C. D.; Yang, H. H. *J. Appl. Polym. Sci.* **1987**, *33*, 1199.
(4) (a) Wu, S. *J. Polym. Sci., Polym. Phys. Ed.* **1987**, *25*, 557, 2511. (b) Wu, S. *Polymer* **1987**, *28*, 1144.
(5) Colby, R. H. *Polymer* **1989**, *30*, 1275.
(6) Roover, J.; Toporowski, P. M. *Macromolecules* **1992**, *25*, 1096, 3454.
(7) Aoki, Y. *Macromolecules* **1990**, *23*, 2309.
(8) Han, C. D.; Kim, J. K. *Macromolecules* **1989**, *22*, 1914, 4292.
(9) Han, C. D.; Chung, H. S.; Kim, J. K. *Polymer* **1992**, *33*, 546.
(10) Kim, J. K.; Han, C. D.; Lee, Y. J. *Polym. J.* **1992**, *24*, 205.
(11) Yang, H. H.; Han, C. D.; Kim, J. K. *Polymer* **1994**, *35*, 1503.
(12) Caville, J. Y.; Perez, J.; Jourdan, C.; Johari, G. P. *J. Polym. Sci., Polym. Phys. Ed.* **1987**, *25*, 1847.
(13) Stadler, P. F.; Feitas, L.L.; Krieger, V.; Klotz, S. *Polymer* **1988**, *29*, 1643.
(14) Ajji, A.; Choplin, L.; Prud'homme, R. E. *J. Polym. Sci., Polym. Phys. Ed.* **1988**, *26*, 2279; **1991**, *29*, 1573.
(15) Schneider, H. A.; Wirbser, J. *New Polym. Mater.* **1990**, *2*, 149.
(16) Kapnistos, M.; Hinrichs, A.; Vlassopoulos, D.; Anastasiadis, S. H.; Stammer, A.; Wolf, B. A. *Macromolecules* **1996**, *29*, 7155.
(17) Paul, D. R., Newman, S., Eds. *Polymer Blends*; Academic Press: New York, 1978.
(18) Molnar, A.; Eisenberg, A. *Macromolecules* **1992**, *25*, 5774.
(19) Stoelting, J.; Karasz, F. E.; MacKnight, W. J. *Polym. Eng. Sci.* **1970**, *10*, 123.
(20) Here miscibility refers to the definition that a blend exhibits a single T_g.
(21) Roland, C. M.; Ngai, K. L. *Macromolecules* **1991**, *24*, 2261, 5315.
(22) Chung, G.-C.; Kornfield, J. A.; Smith, S. D. *Macromolecules* **1994**, *27*, 964, 5729.
(23) Zawada, J. A.; Ylitalo, C. M.; Fuller, G. G.; Colby, R. H.; Long, T. E. *Macromolecules* **1992**, *25*, 2896.
(24) Zawada, J. A.; Fuller, G. G.; Colby, R. H.; Fetters, L. J.; Roover, J. *Macromolecules* **1994**, *27*, 6851, 6861.
(25) Arendt, B. H.; Krishnamoorti, R.; Kannan, R. M.; Zawail, M.; Kornfield, J. A.; Smith, S. D. *Polym. Mater. Sci. Eng.* **1994**, *71*, 471.
(26) Kim, E.; Kramer, E. J.; Osby, J. O. *Macromolecules* **1995**, *28*, 1979.
(27) Kim, E.; Kramer, E. J.; Wu, W.; Garrett, P. D. *Polymer* **1994**, *35*, 5706.
(28) Lau, S. F.; Pathak, J.; Wunderlich, B. *Macromolecules* **1982**, *15*, 1278.
(29) Saeki, S.; Cowie, J. M. G.; McEwen, I. J. *Polymer* **1983**, *24*, 60.
(30) Cowie, J. M. G.; McEwen, I. J. *Polymer* **1985**, *26*, 1662.
(31) Lin, J. L.; Roe, R. J. *Polymer* **1988**, *29*, 1227.
(32) Widmaier, J. M.; Mignard, G. *Eur. Polym. J.* **1987**, *23*, 989.
(33) Lin, J. L.; Roe, R. J. *Macromolecules* **1987**, *20*, 2168.
(34) Nishi, T.; Wang, T. T.; Kwei, T. K. *Macromolecules* **1975**, *8*, 227.
(35) Nishi, T.; Kwei, T. K. *Polymer* **1975**, *16*, 285.
(36) Yang, H.; Shibayama, M.; Stein, R. S.; Shimizu, N.; Hashimoto, T. *Macromolecules* **1986**, *19*, 1667.
(37) David, D. D.; Kwei, T. K. *J. Polym. Sci., Polym. Phys. Ed.* **1980**, *18*, 2337.
(38) Okada, M.; Han, C. C. *J. Chem. Phys.* **1986**, *85*, 5317.
(39) Han, C. C.; Okada, M.; Muroga, Y.; McCrackin, F. L.; Bauer, B. J.; Tran-Cong, Q. *Polym. Eng. Sci.* **1986**, *26*, 3.
(40) Shibayama, M.; Yang, H.; Stein, R. S.; Han, C. C. *Macromolecules* **1985**, *18*, 2179.
(41) Han, C. C.; Okada, M.; Muroga, Y.; Bauer, B. J.; Tran-Cong, Q. *Polym. Eng. Sci.* **1986**, *26*, 1208.
(42) Kim, J. K.; Han, C. D. *Macromolecules* **1992**, *25*, 271.
(43) Lindner, H. S.; Wilson, W. W.; Mays, J. W. *Macromolecules* **1988**, *21*, 3304.
(44) Richardson, M. J.; Savill, N. G. *Polymer* **1977**, *18*, 3.
(45) Cowie, J. M. G.; Toporowski, P. M. *J. Macromol. Sci., Phys.* **1969**, *B3*, 81.
(46) Neumann, C.; Loveday, D. R.; Abetz, V.; Stadler, R. *Macromolecules* **1998**, *31*, 2493.
(47) Here, logarithmic plots of G' versus G'' are referred to as Han plots for the reasons that it is Han who in 1982 first reported that log G' versus log G'' plots show temperature independence for homopolymers.[48] The Han plot has as its basis a molecular viscoelasticity theory for monodisperse homopolymers.[49a] and also for polydisperse homopolymers.[49b] It should be pointed out that the Han plots has *no* relation whatsoever to the Cole−Cole plot,[50] because the Cole−Cole plot is prepared in rectangular coordinates and it is strictly an empirical correlation suggested for low molecular weight liquids.
(48) Han, C. D.; Lem, K. W. *Polym. Eng. Rev.* **1982**, *2*, 135.
(49) (a) Han, C. D.; Jhon, M. S. *J. Appl. Polym. Sci.* **1986**, *32*, 3809. (b) Han, C. D.; Kim, J. K. *Macromolecules* **1989**, *22*, 4292.
(50) Cole, K. S.; Cole, R. H. *J. Chem. Phys.* **1941**, *9*, 341.
(51) Doi, M.; Edwards, S. F. *The Theory of Polymer Dynamics*; Clarendon Press: Oxford, U.K., 1986.

(52) (a) Han, C. D.; Kim, J. *J. Polym. Sci., Polym. Phys. Ed.* **1987**, *25*, 1741. (b) Han, C. D.; Kim, J.; Kim, J. K. *Macromolecules* **1989**, *22*, 383. (c) Han, C. D.; Baek, D. M.; Kim, J. K. *Macromolecules* **1990**, *23*, 561. (d) Han, C. D.; Baek, D. M.; Kim, J. K.; Ogawa, T.; Sakamoto, N.; Hashimoto, T. *Macromolecules* **1995**, *28*, 5043.

(53) (a) Kim, S. S.; Han, C. D. *Macromolecules* **1993**, *26*, 6633. (b) Kim, S. S.; Han, C. D. *J. Rheol.* **1993**, *37*, 847. (c) Kim, S. S.; Han, C. D. *Polymer* **1994**, *35*, 9. (d) Han, C. D.; Kim, S. S. *Macromolecules* **1995**, *28*, 2089. (e) Mather, P. T.; Romo-Uribe, A.; Han, C. D.; Kim, S. S. *Macromolecules* **1997**, *30*, 7977.

(54) de Gennes, P.-G. *Scaling Concept in Polymer Physics*; Cornell University Press: Ithaca, NY, 1979.

(55) Onuki, A. *J. Chem. Phys.* **1987**, *87*, 3692.

(56) (a) Müller, G.; Stadler, R.; Schlick, S. *Makromol. Rapid Commun.* **1992**, *13*, 117. (b) Müller, G.; Stadler, R.; Schlick, S. *Macromolecules* **1994**, *27*, 1555.

MA980623L